

Depth dependence of iron diffusion in Fe₃Si studied with nuclear resonant scattering

Daniel Kmiec,* Bogdan Sepiol, Marcel Sladeczek, Marcus Rennhofer, Svetoslav Stankov,† and Gero Vogl
Fakultät für Physik, Universität Wien, Strudlhofgasse 4, A-1090 Wien, Austria

Bart Laenens and Johan Meersschaut
Instituut voor Kern- en Stralingsfysica, K.U. Leuven, Celestijnenlaan 200D, B-3001 Leuven, Belgium

Tomasz Ślęzak and Marcin Zając
*Faculty of Physics and Applied Computer Science, AGH University of Science and Technology,
 al. Mickiewicza 30, 30-059 Kraków, Poland*

(Received 12 September 2006; revised manuscript received 4 December 2006; published 26 February 2007)

The access to x-rays of third generation synchrotron radiation sources enables studies of dynamics in metallic systems. The nuclear resonant scattering (NRS) method provides information about elementary atomic jumps. When used in grazing incidence geometry, the sensitivity of the NRS method can be tuned to the surface region. This makes the method especially useful for thin film investigations. Contrary to other surface sensitive methods this technique is not only limited to the surface itself: it allows to retrieve the depth profile of diffusivity from the surface down to the bulk region of the measured sample. Fe-Si intermetallic films with a $D0_3$ structure and close to the stoichiometric Fe₃Si composition have been prepared on an MgO (100) substrate. The NRS measurements in grazing incidence geometry yielded maximum iron diffusivity at the surface and diminishing continuously with the depth. The depth and temperature dependence have been measured and compared with the bulk values.

DOI: [10.1103/PhysRevB.75.054306](https://doi.org/10.1103/PhysRevB.75.054306)

PACS number(s): 68.35.Fx, 66.30.Lw, 33.25.+k

I. INTRODUCTION

The intermetallic Fe₃Si phase is of technical interest due to the wide range of its potential applications connected mainly with its magnetic properties. The combination of magnetic and semiconducting material opens up a new pathway in the development of semiconductor devices utilizing the spin of the carrier.¹ Fe₃Si is just important as a part of a ferromagnet-semiconductor hybrid structure. From the viewpoint of the spintronic device structures, it is highly desirable to explore epitaxial ferromagnet/semiconductor heterostructures that possess a rather perfect interface structure as well as high thermal stability.

Recently, numerous studies of epitaxial growth and long-range order of Fe₃Si on GaAs (Refs. 2–4) or of Fe₃Si hybrid structures on Si(111) surface⁵ have been performed searching for alternative materials of better thermal stability and improved interface quality as desirable for spintronic applications. It is well known that the high-temperature behavior of bulk metals and alloy films is determined by the diffusion of atoms.⁶ Even more important is the role of diffusion in the growth and the stability of thin films. In order to successfully finalize an important step toward the integration of magnetism into microelectronics by the successful growth of high-quality epitaxial ferromagnetic films on semiconductor substrates it is, therefore, very important to investigate processes taking place in the near-surface regions of thin films.

It has been recently demonstrated that the Fe₃Si films are thermally stable to *ex situ* annealing at least up to 670 K,⁷ due to other studies to at least 1170 K.⁸ These properties make Fe₃Si a very good alternative to elemental ferromagnets.

Fe-rich Fe₃Si is known for very fast diffusion of Fe. The Fe diffusion is strongly composition dependent and reaches

its maximum at the stoichiometry. The bulk Fe₃Si system was extensively studied using quasielastic Mössbauer spectroscopy,⁹ tracer diffusion method,¹⁰ and nuclear resonant scattering (NRS) (Ref. 11) of synchrotron radiation.

The very large asymmetry in the diffusivity of the major (Fe) and the minor (Si) component indicates that iron diffusion takes place via nearest-neighbor (NN) jumps between the Fe sublattices.¹² The major role in diffusion play thermal vacancies, which are the main defects in this system.^{13,14} The concentration of antisite atoms increases with higher Si content.¹⁵ From Ref. 16 it is known that the deviations in Si content in both directions from the stoichiometric composition decrease the diffusivity. Randl *et al.*¹⁷ showed that the vibrational density of phonon states cannot be responsible for the pronounced change of the iron diffusivity with composition. A consistent set of diffusion coefficients was obtained from the tracer experiments^{10,12} and from Mössbauer and NRS methods.^{9,11} As shown by Sepiol *et al.*¹¹ and Thiess *et al.*¹⁸ the diffusion of iron atoms in Fe₃Si is very fast and can be observed by NRS just above the Curie temperature $T_C=823$ K.¹⁹ Extending the NRS method with the grazing incidence geometry yields information not only about the bulk sample, but also about the depth dependence of the diffusion coefficient. Since this geometry was successfully applied by Sladeczek *et al.*²⁰ in Fe film on MgO substrate, we used it to investigate diffusion of iron in Fe₃Si.

II. SAMPLE PREPARATION

The $D0_3$ phase is a cubic structure consisting of four interpenetrating fcc sublattices, usually labeled α_1 , α_2 , γ , and β . Three of them (α_1 , α_2 , and γ) are occupied by iron atoms and the β sublattice is occupied by silicon atoms. Each sub-

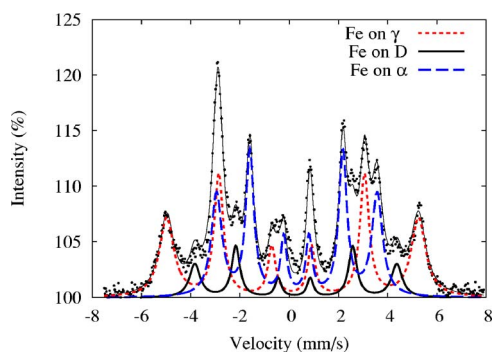


FIG. 1. (Color online) The CEMS spectra of the sample. The stoichiometry of the sample is 77% of Fe and 23% of Si. The solid line is the fit to the data, three components (Lorentzian sextets) result from Zeeman components of iron atoms on α , on γ , and D sites. D sites are α sites but with additional iron atom on the β sublattice in the NN shell—compare sextets corresponding to lowest (around 21 T), highest (31 T), and medium (25 T) magnetic fields, respectively.

lattice is shifted from the neighbor sublattice by 1/4 lattice constant in the diagonal direction. Crystals of Fe_3Si are very well ordered¹⁷ up to the melting point $T_m = 1493$ K. Diffusion of iron atoms in Fe_3Si is one of the fastest of all known intermetallic phases. Former Mössbauer and NRS experiments on Fe_3Si bulk samples^{9,11,21} revealed diffusion mechanism of iron facilitating the present measurements of thin film surfaces.

One of the main difficulties encountered throughout the studies of iron silicide films are rather challenging sample preparation procedures. Whereas production of ϵ - FeSi or FeSi_2 phases is well documented,^{22–24} Fe_3Si thin films are especially difficult in preparation. Ordered iron silicide films were prepared on an $\text{MgO}(001)$ substrate by molecular beam epitaxy (MBE). The thickness of the MgO substrate was 0.5 mm. The samples were prepared under UHV conditions by layer-by-layer deposition of iron and silicon layers in the proportion close to the ordered $D0_3$ structure of Fe_3Si (3:1). The deposition was done at ≈ 470 K. The reflectivity measurement revealed only thickness oscillations from a homogeneous Fe-Si layer.

The sample was transported in inert atmosphere to the synchrotron and loaded via a glove-bag into a load-lock system of an UHV chamber. (For a detailed description of the chamber see Ref. 25.)

The sample was characterized by conversion electron Mössbauer spectroscopy (CEMS) and x-ray diffraction (XRD) before and after the NRS experiment. Stoichiometry of the film could be determined directly from CEMS spectra yielding 77(1)% of Fe and 23(1)% of Si.^{26,27} The measured spectrum and the appropriate fit is shown in Fig. 1.

XRD measurements (see Fig. 2) confirmed the well ordered intermetallic phase with the (001) axis perpendicular to the surface. In order to check the in-plane thin layer quality a grazing incidence diffraction (GID) measurement has been performed. The sample was well in-plane ordered [see Fig. 2(b)]. [100] and [010] lattice directions were parallel to [110] and $[1\bar{1}0]$ directions of the MgO substrate, respectively. From the width of the GID peak we estimate domains

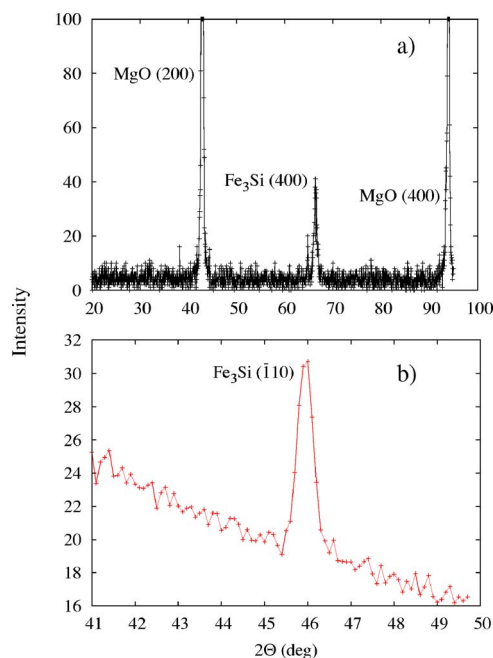


FIG. 2. (Color online) (a) X-ray diffraction spectrum from $\text{Fe}_{77}\text{Si}_{23}$ measured in the specular geometry (the y axis shows values up to 100 counts). (b) The GID intensity from the $(\bar{1}10)$ lattice planes perpendicular to the sample surface.

with the mean dimension over 200 nm. Thus the sample will be further regarded as a single crystal. The sample thickness measured by x-ray reflectivity was 15 ± 1 nm.

III. EXPERIMENT

A. Measurements

NRS in the time domain can be used for measurement of atomic jumps as was theoretically shown by Smirnov and Kohn.^{28,29} The NRS method exploits the excitation of iron atoms into a high-energy state. The response of the sample is measured by fast electronics (APD detectors). The spectrum consists of two parts. The first part comes from photons scattered by electrons (ps time scale). The second part are photons re-emitted after resonant absorption providing information about dynamics in the sample. Combination with the grazing incidence geometry shows an enhancement of the surface sensitivity of the method and enables studies of diffusion in bulk and in near-surface regions.

The thermal treatment of the sample was realized by means of resistivity heating in a Mo-sample holder. The substrate was a 10×10 mm polished MgO crystal. The temperature of the Mo holder was controlled by a thermocouple attached to its surface. In order to estimate the temperature offset between the surface of the Mo holder and the surface of the Fe-Si layer, the layer temperature was calibrated by the magnetic transition (ferromagnetic-paramagnetic) of the Fe_3Si film [$T_C = 823$ K (Ref. 19)]. The ferromagnetic-paramagnetic transition was clearly visible in the forward scattering intensity as a sharp intensity drop (increase), when changing temperature below (above) Curie temperature, respectively.

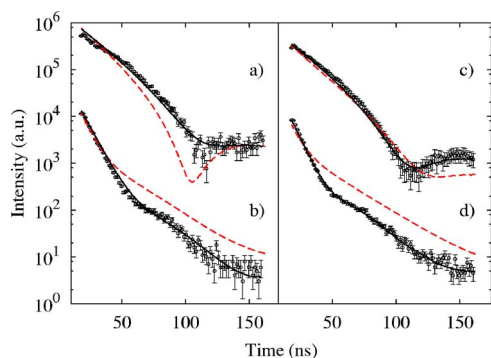


FIG. 3. (Color online) NRS spectra for two different incidence angles at $T=873$ K: (a) $\alpha=2.47$ mrad, (b) $\alpha=3.70$ mrad and at $T=923$ K: (c) $\alpha=2.47$ mrad, (d) $\alpha=3.70$ mrad. The solid lines represent best fits with the model where the boundary between the bulk layer and the adjacent near-surface layer lies at 3.5 nm. The dashed (red) lines represent best fits achieved with the bulk model (constant diffusion along sample depth).

NRS investigations were performed at the ID18 beamline at ESRF in Grenoble operating in 16-bunch timing mode in the standard setup for grazing incidence geometry.³⁰ The vertical dimension of the beam was $150 \mu\text{m}$. The sample was kept under UHV conditions in a chamber dedicated for grazing incidence investigation and mounted on a two circle goniometer during measurements.

To avoid a very demanding interpretation of the beat pattern in the NRS spectra resulting from magnetic hyperfine interactions,³¹ the diffusion investigations have been carried out above the Curie temperature of Fe_3Si . The NRS measurements were performed in grazing incidence geometry at several temperatures above T_C and at two different incidence angles (2.47 and 3.70 mrad). Enhanced diffusion in the sample results in an acceleration of the re-emitted intensity,^{11,29,32,33} which allows us to extract information about diffusion from the NRS spectra.

B. Data evaluation

The measured spectra were evaluated with the EFFINO software.³⁴ The theoretical background of the forward and grazing incidence geometry for both energy and time domain spectra offered by the program can be found in Ref. 35. The software has been chosen for fitting because it allows implementing several distinct iron sites within one layer, which is necessary for the used model. Thanks to a combination of EFFINO and scripts written by the author we could realize depth profiles by preparing appropriate input files. None of the available fitting routines can otherwise attain this goal. It turned out impossible to fit the data with only one 15 nm thick Fe_3Si bulk layer (see dashed lines in Fig. 3) and also with enhanced diffusion limited to the sample surface only. Thus the sample was modelled as a layered structure containing 11 layers. The topmost ten layers modelled the near-surface part of the sample. The eleventh layer was a bulk layer. This is an extension of the model used by Sladeczek *et al.*,²⁰ where the sample is described by two layers only with a stepped diffusivity profile on the boundary between the

near-surface region and the bulk. The use of more layers allows one to model a smooth diffusivity profile from top to bulk. The depth profiles were realized by means of the Fermi-like function $f(d)=1/[1+\exp(d-d_0)/\sigma^2]$, where d denotes the sample depth and d_0 and σ define the position and the shape of the profile. This model is chosen as a natural extension of the “two-layer model.” In contrast to the one- or two-layer models this one fits successfully the measured data and—what is also important—it describes the sample in a more realistic way. In each layer parameters such as Lamb-Mössbauer factor or diffusion coefficient can be set independently. Such an approach allows to identify different diffusion coefficients at different sample depths which leads to a diffusion-depth profile. The bulk diffusion model of iron in Fe_3Si of Sepiol *et al.*^{9,11,36} with two distinct iron sites (α and γ) with different weights was chosen for the fitting. *Ab initio* calculations using first principle density-functional theory on the $D0_3 \text{Fe}_3\text{Si}$ system have been performed recently.³⁷ These calculations completely confirmed the α - γ jump model.^{9,36} The calculated activation energies for the diffusion of Fe show much smaller values for the jumps along $\langle 111 \rangle$ direction. The activation energy for this process is only 0.59 eV compared to 2.42 eV for jumps along $\langle 100 \rangle$ (α_1 - α_2 jumps),³⁷ and is in perfect agreement with the experiment.^{9,33,36} The enhanced diffusivity in the near-surface region of the film was necessary in order to get satisfying fits. All spectra measured at the same temperature were fitted simultaneously with constant total thickness of the sample, whereas the boundary between the near-surface region and the bulk part of the film was allowed to move. Each spectrum has assigned particular incidence angle and intensity. Only these two parameters are not shared between the spectra at given temperature.

The one- or two-layer structures could be immediately classified as false models for iron diffusion near the Fe_3Si surface. An exponential dependence of the diffusivity was tested without success. Probably this function is too steep and the contribution of the surface to the spectrum is underestimated. The Fermi-like model is an “intelligent guess” providing, in our opinion, good estimation of the depth dependence of iron diffusivity. We can not claim, however, that the Fermi-like model is the only possible solution. The NRS spectra are not sensitive enough to enable distinction between functions similar to the Fermi-like function.

IV. RESULTS AND DISCUSSION

Typical NRS spectra measured at 873 K and for an incidence angle of (a) $\alpha=2.47$ mrad and (b) $\alpha=3.70$ mrad (b) are shown in Fig. 3. The dashed lines are shown for comparison and represent the best fits achieved with constant diffusion along the sample depth.

The best fit with the measured data was reached with the interface between the near surface and the bulk lying between 3 and 3.5 nm depth. The fits show very strong diffusion depth dependence in the near-surface region. The diffusion depth profiles for three measured temperatures are presented in Fig. 4.

The measurements show depth dependence of the diffusivity in the whole measured range. The diffusivity in the

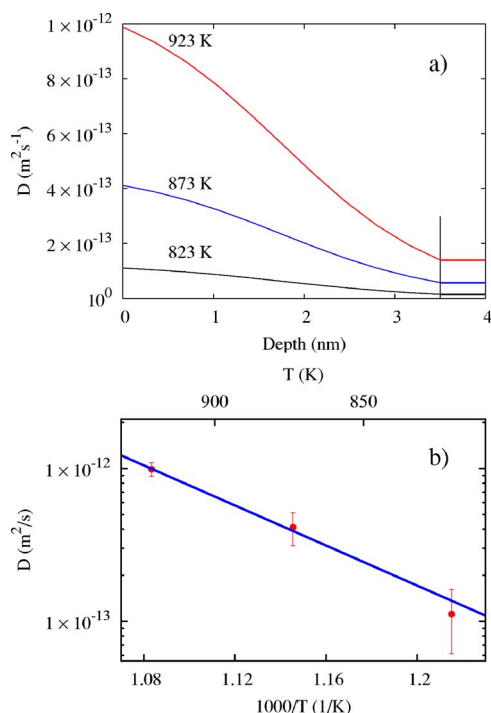


FIG. 4. (Color online) Diffusion-depth profiles for three measured temperatures. The vertical line denotes the assumed boundary between the near-surface and the bulk region (a). Arrhenius plot of the diffusivity in the near-surface layer at three measured temperatures. The activation energy is $E_A = 1.30 \pm 0.12$ eV and the pre-exponential factor is $D_0 \approx 2 \times 10^{-5} \text{ m}^2 \text{ s}^{-1}$ (b).

top-most part of the thin film is faster than in the bulk and decreases slowly reaching the values of bulk at approximately 3 to 3.5 nm. The diffusivity increases with temperature [see Fig. 4(b)], the activation energy for the near-surface layer is about 1.30 eV, and the pre-exponential factor $D_0 = 2 \times 10^{-5} \text{ m}^2 \text{ s}^{-1}$. The activation energy near the sample surface is lower than the corresponding value extrapolated from tracer data of Gude and Mehrer¹⁰ for the composition of $\text{Fe}_{77}\text{Si}_{23}$ $E_A \approx 1.77$ eV. The pre-exponential factor is in good agreement with that of the tracer bulk sample. The reduction of the activation energy for diffusion in the near-surface layer was also observed in pure α -iron measured by Sladeczek *et al.*³⁸

An enhanced diffusivity in the uppermost atomic layers of α -Fe³⁸ indicates that this effect is not connected with the alloy disorder on the sample surface. From the high-temperature measurements of Starke *et al.*⁸ it is known that the uppermost layer of the $D\text{O}_3$ phase is modified, but this

reversible reconstruction process concerns only the first layer which has a nearly negligible impact on the NRS spectrum. One shall note that the penetration depth of the synchrotron radiation, i.e., the thickness where the amplitude of the electric field decays to a fraction of $1/e$, is much larger than a few monolayers. For example, the penetration depths for $\text{Fe}_{77}\text{Si}_{23}$ are 2.3 and 5.8 nm for incidence angles of 2.47 and 3.70 mrad, respectively.

There is no other experimental method which can measure diffusion close to the surface. Methods such as inelastic helium atom scattering³⁹ (HAS) or scanning tunneling microscopy (STM) are limited to the uppermost surface layer only and are not able to look deeper into the sample. On the other hand theoretical *ab initio* calculations are limited to a small number of atoms (≈ 100), which in some cases may be enough for surface calculations, but not for depth profiles reaching from surface to bulk. A different approach, the Green function method, can simulate more atomic layers and can be useful for depth calculations providing some pure metals atomic relaxation of 20–30 layers (\approx few nm).⁴⁰

V. CONCLUSIONS

Diffusivity measurements in near stoichiometric Fe_3Si films were performed by means of nuclear resonant scattering in grazing incidence geometry. The measurements show a depth and temperature dependence of iron diffusion in $\text{Fe}_{77}\text{Si}_{23}$. The experiment revealed enhanced diffusivity in the near-surface region decreasing with the sample depth. The boundary between regions of enhanced surface diffusion and bulk diffusion lies approximately at 3.5 nm. The bulk diffusion values are in good agreement with tracer data. We conclude that for depth diffusion studies in thin film, depth profiling grazing incidence geometry NRS appears to be an effective tool.

ACKNOWLEDGMENTS

This work was supported by grants of the Austrian *Fonds zur Förderung der wissenschaftlichen Forschung* contract P-17775-N02, the 6th framework program of the European Union No. 001516 (DYNASYNC), and by bm:bwk GZ 45.529/2-VI/B/7a/2002 (MDN). The measurement time at the X-ray diffractometer provided by Erhard Schafner (University of Vienna) is also acknowledged. We thank Peter Seebacher (University of Vienna) for the support during GID measurements and Janusz Przewoznik (AGH University of Science and Technology) for XRD measurements. J. Meerss-chaut thanks the Research Fund K.U. Leuven for the financial support.

*Electronic address: daniel.kmiec@univie.ac.at

†Also at European Synchrotron Radiation Facility, 6 Rue Jules Horowitz, BP220 38043 Grenoble Cedex, France

¹G. A. Prinz, *Science* **282**, 1660 (1998).

²A. Ionescu *et al.*, *Phys. Rev. B* **71**, 094401 (2005).

³P. Muduli, J. Herfort, H.-P. Schönherr, and K. Ploog, *J. Cryst. Growth* **285**, 514 (2005).

⁴B. Jenichen, V. M. Kaganer, J. Herfort, D. K. Satapathy, H. P. Schönherr, W. Braun, and K. H. Ploog, *Phys. Rev. B* **72**, 075329 (2005).

- ⁵K. Kobayashi, T. Sunohara, M. Umada, H. Yanagihara, E. Kita, and T. Suemasu, *Thin Solid Films* **508**, 78 (2006).
- ⁶H. Mehrer, in *Diffusion in Condensed Matter*, edited by P. Heitjans and J. Kärger (Springer, Berlin, 2005), pp. 3–63.
- ⁷J. Herfort, H.-P. Schönherr, A. Kawaharazuka, M. Ramsteiner, and K. Ploog, *J. Cryst. Growth* **278**, 666 (2005).
- ⁸U. Starke, W. Meier, C. Rath, J. Schardt, W. Weiß, and K. Heinz, *Surf. Sci.* **377–379**, 539 (1997).
- ⁹B. Sepiol and G. Vogl, *Phys. Rev. Lett.* **71**, 731 (1993).
- ¹⁰A. Gude and H. Mehrer, *Philos. Mag. A* **76**, 1 (1997).
- ¹¹B. Sepiol, A. Meyer, G. Vogl, R. Ruffer, A. I. Chumakov, and A. Q. R. Baron, *Phys. Rev. Lett.* **76**, 3220 (1996).
- ¹²H. Mehrer, M. Eggersmann, A. Gude, M. Salamon, and B. Sepiol, *Mater. Sci. Eng., A* **239–240**, 889 (1997).
- ¹³H.-E. Schaefer and K. Badura-Gergen, *Defect Diffus. Forum* **143–147**, 193 (1997).
- ¹⁴E. A. Kümmerle, K. Badura, B. Sepiol, H. Mehrer, and H.-E. Schaefer, *Phys. Rev. B* **52**, R6947 (1995).
- ¹⁵A. Broska, J. Wolff, M. Franz, and T. Hehenkamp, *Intermetallics* **7**, 259 (1999).
- ¹⁶H. Thiess, B. Sepiol, R. Ruffer, and G. Vogl, *Defect Diffus. Forum* **194–199**, 363 (2001).
- ¹⁷O. G. Randl, G. Vogl, W. Petry, G. Hennion, B. Sepiol, and K. Nembach, *J. Phys.: Condens. Matter* **7**, 5983 (1995).
- ¹⁸H. Thiess, M. Kaisermayr, B. Sepiol, M. Sladeczek, R. Ruffer, and G. Vogl, *Phys. Rev. B* **64**, 104305 (2001).
- ¹⁹T. B. Massalski, *Binary Alloy Phase Diagrams* (American Society for Metals, Metals Park, Ohio, 1986).
- ²⁰M. Sladeczek, B. Sepiol, M. Kaisermayr, J. Korecki, B. Handke, H. Thiess, O. Leupold, R. Ruffer, and G. Vogl, *Surf. Sci.* **507–510**, 124 (2002).
- ²¹B. Sepiol, A. Meyer, G. Vogl, H. Franz, and R. Ruffer, *Phys. Rev. B* **57**, 10433 (1998).
- ²²B. Croonenborghs, F.-M. Almeida, S. Cottenier, M. Rots, A. Vantomme, and J. Meersschat, *Appl. Phys. Lett.* **85**, 200 (2004).
- ²³S. Degroote, A. Vantomme, J. Dekoster, and G. Langouche, *Appl. Surf. Sci.* **91**, 72 (1995).
- ²⁴M. Fanciulli, G. Weyer, A. Svane, N.-E. Christensen, H. von Kanel, E. Muller, N. Onda, L. Miglio, F. Tavazza, and M. Celino, *Phys. Rev. B* **59**, 3675 (1999).
- ²⁵M. Sladeczek, Ph.D. thesis, University of Vienna, 2005, available at http://homepage.univie.ac.at/Marcel.Sladeczek/phd/PhD_Sladeczek.pdf
- ²⁶G. Rixecker, P. Schaaf, and U. Gonser, *Phys. Status Solidi A* **139**, 309 (1993).
- ²⁷L. K. Varga, F. Mazaleyrat, J. Kovac, and J. M. Greneche, *J. Phys.: Condens. Matter* **14**, 1985 (2002).
- ²⁸G. V. Smirnov and V. G. Kohn, *Phys. Rev. B* **52**, 3356 (1995).
- ²⁹V. G. Kohn and G. V. Smirnov, *Phys. Rev. B* **57**, 5788 (1998).
- ³⁰R. Ruffer and A. Chumakov, *Hyperfine Interact.* **97/98**, 589 (1996).
- ³¹G. V. Smirnov, *Hyperfine Interact.* **123/124**, 31 (1999).
- ³²G. Vogl and B. Sepiol, *Hyperfine Interact.* **123/124**, 595 (1999).
- ³³G. Vogl and B. Sepiol, in *Diffusion in Condensed Matter*, edited by P. Heitjans and J. Kärger (Springer, Berlin, 2005), pp. 65–91.
- ³⁴H. Spiering, L. Deák, and L. Bottyán, *Hyperfine Interact.* **125**, 197 (2000).
- ³⁵L. Deák, L. Bottyán, D. L. Nagy, and H. Spiering, *Phys. Rev. B* **53**, 6158 (1996).
- ³⁶B. Sepiol and G. Vogl, *Hyperfine Interact.* **59**, 149 (1995).
- ³⁷S. Dennler and J. Hafner, *Phys. Rev. B* **73**, 174303 (2006).
- ³⁸M. Sladeczek, B. Sepiol, J. Korecki, T. Slezak, R. Ruffer, D. Kmiec, and G. Vogl, *Surf. Sci.* **566–568**, 372 (2004).
- ³⁹A. P. Graham, *Surf. Sci. Rep.* **49**, 115 (2003).
- ⁴⁰A. Kara and T. S. Rahman, *Surf. Sci. Rep.* **56**, 159 (2005).